

Optical Engineering

OpticalEngineering.SPIEDigitalLibrary.org

Effects of pulsed and continuous-wave laser radiation on the fabrication of tissue-engineered composite structures

Mikhail S. Savelyev
Natalia O. Agafonova
Pavel N. Vasilevsky
Dmitry I. Ryabkin
Dmitry V. Telyshev
Peter S. Timashev
Alexander Yu. Gerasimenko

SPIE.

Mikhail S. Savelyev, Natalia O. Agafonova, Pavel N. Vasilevsky, Dmitry I. Ryabkin, Dmitry V. Telyshev, Peter S. Timashev, Alexander Yu. Gerasimenko, "Effects of pulsed and continuous-wave laser radiation on the fabrication of tissue-engineered composite structures," *Opt. Eng.* **59**(6), 061623 (2020), doi: 10.1117/1.OE.59.6.061623

Effects of pulsed and continuous-wave laser radiation on the fabrication of tissue-engineered composite structures

Mikhail S. Savelyev,^{a,b,*} Natalia O. Agafonova,^a Pavel N. Vasilevsky,^a
Dmitry I. Ryabkin,^a Dmitry V. Telyshev, Peter S. Timashev,^{b,c,d} and
Alexander Yu. Gerasimenko^{a,b}

^aNational Research University of Electronic Technology MIET, Zelenograd, Moscow, Russia

^bI.M. Sechenov First Moscow State Medical University, Moscow, Russia

^cN.N. Semenov Institute of Chemical Physics, Moscow, Russia

^dResearch Center “Crystallography and Photonics,” Troitsk, Moscow, Russia

Abstract. We studied the formation of a composite from an aqueous dispersed medium with albumin and carbon nanotubes under the action of laser radiation in continuous wave (CW) mode and pulsed mode with a repetition rate of 10 Hz and pulse duration of 16 ns. During the experiments, the temperature was monitored at the site of exposure, as well as its distribution in the liquid. Pulsed solid-state Nd:YAG laser and CW diode laser with an irradiation power of ~500 mW were used as radiation sources. However, a three-dimensional composite was formed only with constant exposure. The effect of pulsed laser radiation with an intensity corresponding to nonlinear interaction with water dispersion led only to its enlightenment. Thus, it is important not only the energy parameters of radiation but also the frequency of energy portions exposure for the fabrication of tissue-engineered structures (composites). As a result, it was found that the curing of the dispersion and the composite formation occurs under the action of continuous or pulsed (with a high pulse repetition rate) laser radiation at a temperature in the range from 45°C to 50°C; in case the pulse repetition rate is insufficient, composite formation is not observed even under the action of high intensity radiation and heating occurs only to a temperature of ~40°C. This formation process can be generated both in the visible 532 nm and in the infrared 810-nm wavelength ranges. In this case, one of the main conditions is the absence of albumin or cells absorption at these wavelengths so that absorption occurs mainly with single-walled carbon nanotubes. Studies of the surface and internal structure of the composite made it possible to demonstrate the binding of nanotubes to each other. This happened under the influence of laser radiation. This led to high hardness values of the composites. The average value of hardness was 0.26 ± 0.02 GPa. © 2020 Society of Photo-Optical Instrumentation Engineers (SPIE) [DOI: [10.1117/1.OE.59.6.061623](https://doi.org/10.1117/1.OE.59.6.061623)]

Keywords: pulsed laser radiation; continuous wave; composite; carbon nanotubes; lasers; non-linear optical effect; tissue engineering; bovine serum albumin.

Paper 191529SS received Oct. 31, 2019; accepted for publication Jan. 22, 2020; published online Feb. 11, 2020.

1 Introduction

The main task of tissue engineering is the creation of implantable tissues and organs with sufficient mechanical strength, which are also biocompatible. To achieve this goal, it is necessary to select the initial components, then form and deliver supporting structures and living cells to the damage zone.^{1,2} Such tissue-engineered structures should ultimately lead to the restoration of the necessary functional ability.^{3,4} Therefore, supporting structures called “scaffolds” should provide the necessary conditions for cell fixing and proliferation.^{5,6} For these reasons, albumin⁷ is promising material as a matrix supporter, but additional components must be used to increase its

*Address all correspondence to Mikhail S. Savelyev, E-mail: savelyev@bms.zone

mechanical characteristics.^{8,9} To achieve these requirements, single-walled carbon nanotubes (SWCNTs), which are capable of biodegradation during tissue regeneration,¹⁰⁻¹² can be introduced into the composition of the hydrogel. However, it is impossible to make a broad coverage when classifying carbon nanotubes as “nontoxic” and “toxic” since their effect on cells depends on their application.^{13,14} In general, as in case of other molecules and materials, their effectiveness and side effects depend on the following factors: dose, route of administration, and type of exposure.^{15,16} Various research groups also attempted to develop SWCNTs with specific forms and properties.^{17,18} It has been shown that carbon nanotubes have high hemocompatibility values, the hemolysis level is 5% upon contact with blood.¹⁹ In addition, their use in a solution of proteins, such as serum albumin, reduces the activity of nanotubes to the platelet aggregation.^{20,21} The treatment process of SWCNTs with albumin occurs due to conformational changes in protein structure. In previous research, it was determined that composite films with bovine serum albumin (BSA) and SWCNTs show the absence of hemolysis while contacting with blood.²²

Another important issue concerns the preparation method itself since the properties of the material strongly depend on the surface morphology and its structure as a whole.^{5,23} Promising methods for the formation of tissue-engineered structures is three-dimensional (3-D) printing, based on additive technology for accurate 3-D design.²⁴ The use of stereolithography makes it possible to solidify hydrogels and create the necessary structure with high accuracy. Nevertheless, the main disadvantage of this method is the use of ultraviolet radiation sources, the effects of which are harmful to cells and can cause skin cancer.^{24,25} The possibility of curing a liquid dispersed medium (hydrogel) in the infrared²⁶ and the visible wavelength range²⁷ was shown. Other authors are also investigating the possibility of using laser radiation that does not lie in the ultraviolet range.^{28,29}

In this work, we study the effect of laser radiation with the same wavelength, but with different irradiation modes, namely, for the case of continuous wave (CW) and high-intensity pulsed radiation. These types of effects are characterized by linear and nonlinear interaction of laser radiation with the material, which can be divided by the threshold intensity value.³⁰ The studies were conducted with hydrogel based on BSA and SWCNTs.

2 Experimental Details

2.1 Fabrication of Dispersions of Carbon Nanotubes with Albumin

Hydrogels are an aqueous dispersed medium of BSA 20% (w/w) with SWCNTs 0.01% (w/w) and without them.

The preparation of the hydrogel was carried out as follows:

- all the components used were weighed on an analytical balance, and in the case of SWCNTs, the proportion of their content in the initial aqueous paste 2.5% (w/w) per 1 g was taken into account;
- BSA aqueous dispersion was prepared without the addition of SWCNTs by mixing in an ultrasonic bath at power of 40 W;
- aqueous dispersion with SWCNTs, which were initially in form of aqueous paste, was mixed using a submersible homogenizer with a power of ~450 W in a graduated glass with a capacity of 50 ml for 3600 s;
- the hydrogel was obtained by mixing both dispersions together in ultrasonic bath.

2.2 Measurement of Nonlinear Optical Properties

Before investigating the curing process, the nonlinear optical properties of the prepared hydrogels were measured to determine the nature of the interaction of laser radiation with matter. To do this, we used the optical scheme and measurement procedure, which had previously been tested in the measurement of SWCNTs conjugates.³¹ This description takes into account only the absorption by the material; however, it can be applied in the case of the combined action of absorption and scattering. A distinctive feature of the study of hydrogel by the fixed sample

location method was the use of a laser beam without focusing, respectively, the spot diameter was ~ 1.5 mm at a level of $1/e^2$. As the initial energy for Z-scanning with an open aperture, a value was chosen at which nonlinear effects do not occur without beam focusing. These studies were carried out only with the use of nanosecond Nd:YAG laser since the intensity of radiation generated by CW laser was not enough to cause nonlinear processes without prolonged exposure to the substance. In the case of hydrogel with SWCNTs, the attenuation of laser radiation is mainly caused by the presence of nanotubes; the absorption of albumin is insignificant during operation in the visible wavelength range.³² The described measurement procedure is used to distinguish between linear and nonlinear interactions in order to select the initial conditions under which the effect of prolonged exposure with temperature control would be studied.

2.3 Temperature and Transmittance Measurements during the Hydrogel Curing

The optical scheme of the experiment for irradiating prepared BSA hydrogel with/without SWCNTs is shown in Fig. 1. The study was conducted in the visible range with a wavelength of laser radiation of 532 nm. The second harmonic of Nd:YAG laser with a single pulse duration of 16 ns and frequency of 10 Hz was used; a solid-state laser with diode pumping was used as a CW radiation source. The results comparison was carried out at the same power for 720 s. The sample was placed in a 2-mm-thick quartz cuvette, which was mounted vertically. The laser beam from the radiation source is incident on the cuvette perpendicularly and hit an Ophir 12 A-P sensor after passing through the hydrogel. The power was maintained constant throughout the irradiation process and was recorded using a beam splitter plate and an Ophir PE9-C sensor. The temperature of the sample at the irradiation site was recorded using an Optris Laser Sight pyrometer operating in a noncontact mode.

The spot diameter of the pulsed solid-state Nd:YAG laser did not exceed 1.1 mm at a $1/e^2$ level. Figure 2 shows a beam profile that was registered by a CCD camera. Similar measurement was performed for the CW diode laser. The diameter of such beam was 2 mm at a $1/e^2$ level.

3 Results

3.1 Characterization of Linear and Nonlinear Optical Properties

To determine the linear and nonlinear optical characteristics, fixed sample location experiment and Z-scanning were performed. Irradiation was performed for 2 s, after which the incident and transmitted powers were recorded. Figure 3(a) shows a graph of the output energy dependence on the input energy, constructed according to the results of fixed sample location experiment. The energy values were calculated taking into account the laser radiation frequency of 10 Hz. To conduct a Z-scanning, a power corresponding to the linear region of the input–output

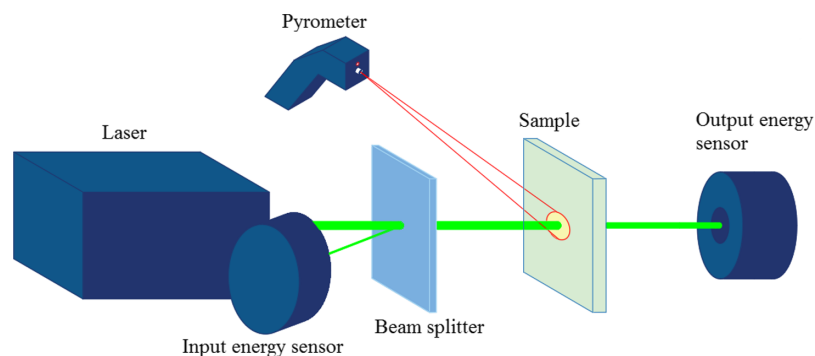


Fig. 1 Experimental scheme.

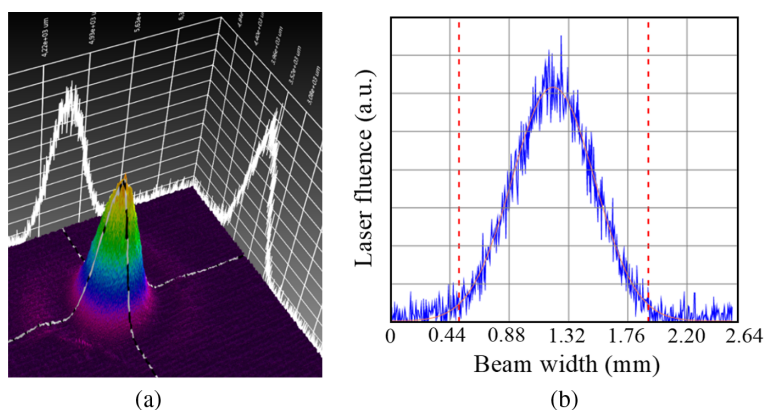


Fig. 2 Laser beam profile: (a) registered by a CCD camera and (b) the projection of this profile along one of the axes, the dashed lines correspond to the attenuation of the peak value in $1/e^2$.

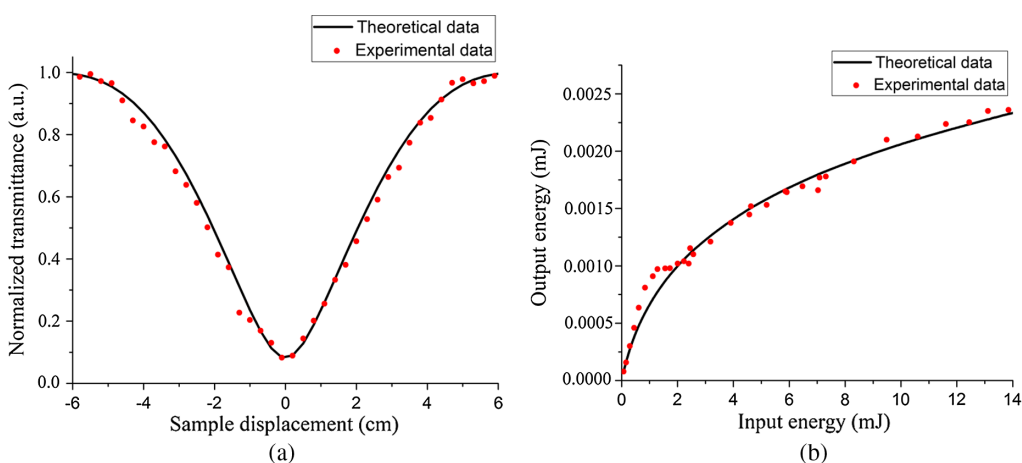


Fig. 3 Experimental and theoretical dependences of: (a) output energy on the incident beam energy; (b) normalized transmittance on the position of the hydrogel sample relative to the lens focus.

dependence curve equals to 4 mW was chosen. Z-scanning [Fig. 3(b)] was performed with a step of 3 mm.

According to the experiments results, theoretical curves were calculated that are in good agreement with the experimental data. The linear absorption coefficient α of the studied hydrogel is 33.62 cm^{-1} . In addition, the hydrogel also exhibits strong nonlinear properties: the nonlinear absorption coefficient β is 53.2 cm/MW at a threshold intensity I^{th} (intensity at which nonlinear absorption effects occur) of 0.487 MW/cm^2 . Such a high β value can be explained by the high concentration of nanotubes² in conjunction with an increase in the temperature of this material.³²

3.2 Long-Term Pulsed and CW Irradiation

Long-term irradiation of a hydrogel based on BSA and SWCNTs was carried out in two modes: pulsed (10 Hz) and CW. The wavelength (532 nm) and the radiation power (500 mW) were the same in both cases.

The time dependences of temperature show different patterns of interaction of the hydrogel with pulsed and CW laser radiation (Fig. 4).

When using continuous radiation, the temperature rather quickly increased to 45°C without any structural changes in sample (I red in Fig. 4), and then slowly increased by 1°C to 1.5°C over

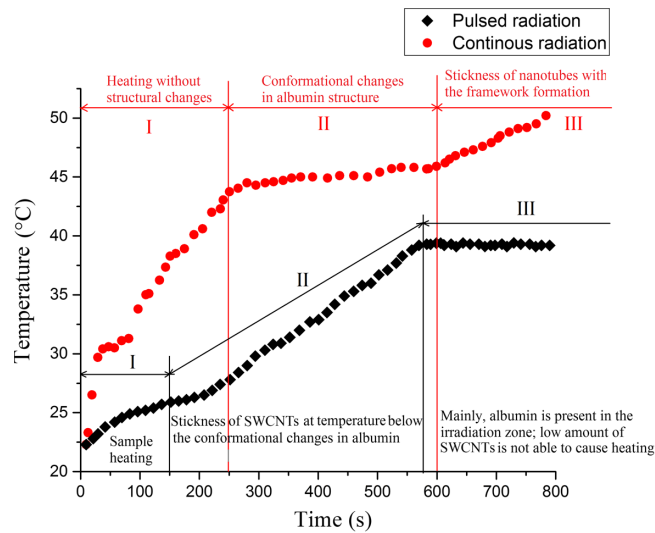


Fig. 4 Time dependence of temperature during long-term irradiation of hydrogel.

the next 360 s (II red). During this period, conformational changes in albumin structure began to occur. Further irradiation led to a composite formation due to the stickiness of nanotubes (III red). Immediately after the beginning of the solid composite formation, the temperature was increasing again. This is due to the fact that the radiation ceased to pass through the liquid medium and most part of radiation was absorbed by the solid composite, heating it.

In the pulsed mode, the main temperature increase was observed from 90 to 600 s of irradiation, which corresponds to the region of enlightenment (II black). However, the maximum temperature of the hydrogel during the irradiation period did not exceed 40°C, from which we can conclude that the temperature of conformational changes in albumin was not reached in this case. Due to sticking, SWCNTs leave the irradiation area and the remaining small amount of SWCNTs is not able to cause heating to higher temperature (III black).

It should be noted that BSA dispersions without SWCNTs did not interact with radiation in both modes. The temperature change over the entire period of irradiation did not exceed 1°C.

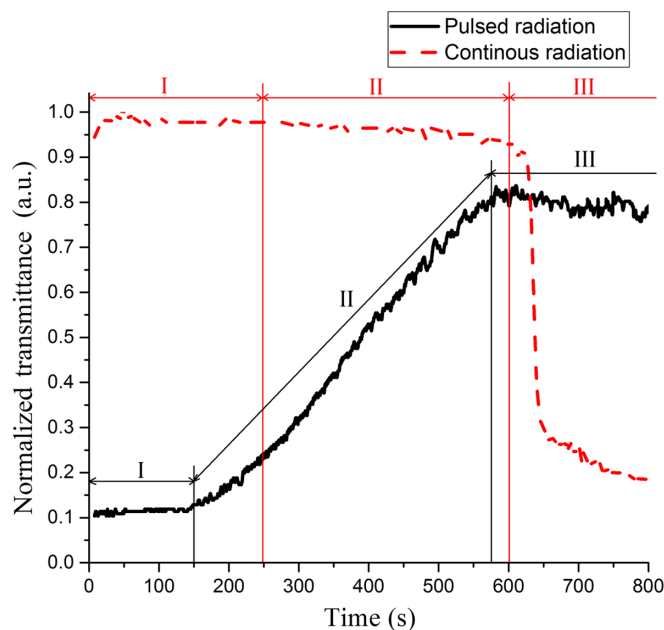


Fig. 5 Time dependence of normalized transmission during long-term irradiation of hydrogel.

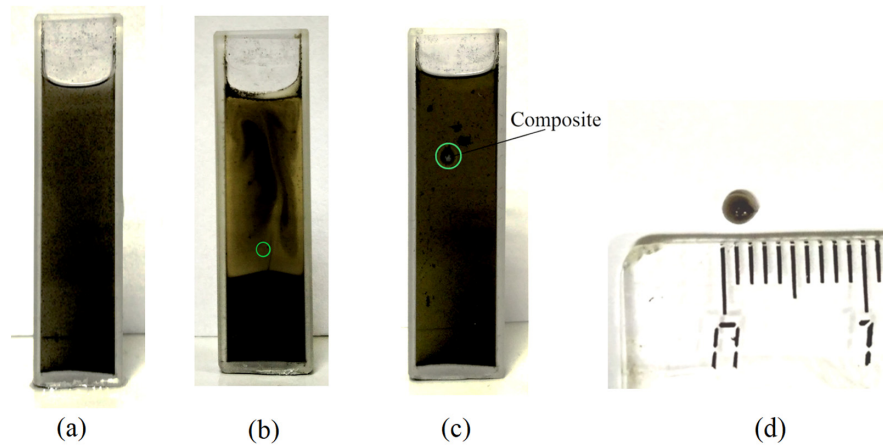


Fig. 6 The shows of hydrogel: (a) before irradiation, (b) after irradiation in pulsed mode, (c) after irradiation in CW mode, and (d) solid composite. The green circles show irradiation areas in both modes.

The dependence of the normalized transmission on time is shown in Fig. 5. During irradiation process in pulsed mode, the hydrogel exhibits nonlinear properties in the initial period of irradiation (\sim the first 120 s). However, then the effect of enlightenment was observed. Due to the presence of nonlinear effects, the value of normalized transmittance did not reach the value of 1, but visually the dispersion became more transparent at the irradiation site and above [Figs. 6(a) and 6(b)]. In turn, the area below the irradiation site becomes visually darker. The normalized transmission growth stopped in 600 s after the start of irradiation. I-III red and I-III black areas correspond to similar areas shown in Fig. 4.

In case of CW radiation, the normalized transmission was close to the value of 1, which indicates the absence of nonlinear effects. The value of normalized transmittance sharply decreased in 600 s, which was associated with solid composite formation [Figs. 6(c) and 6(d)].

3.3 Characteristics of Tissue Engineered Structures (Composite)

Scanning electron microscopy (SEM) was used to determine the surface and internal structure of the composite fabricated using CW irradiation. All images were obtained using a Tescan VEGA3 microscope at an accelerating voltage of the electron column of 30 kV. Before starting the study, the sample was divided into small fragments in size of $\sim 0.5 \text{ mm}^3$. Then, the fragments were washed into powder using an agate mortar. The size of the powder fractions was $\sim 100 \mu\text{m}^3$.

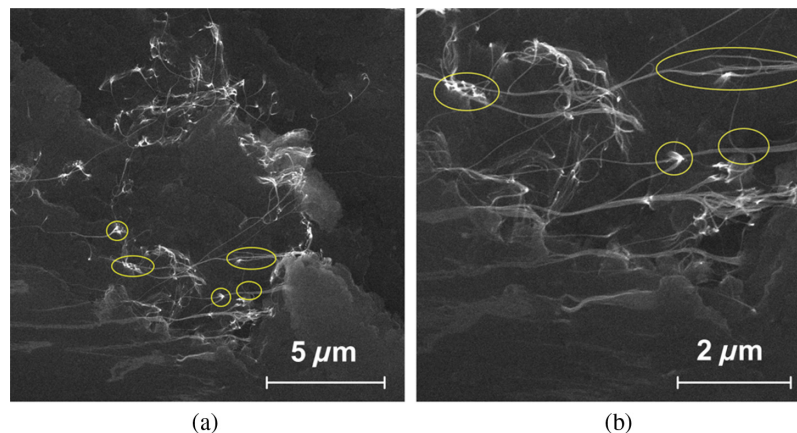


Fig. 7 SEM images of the stretched region of the composite at different scales: (a) overview image and (b) enlarged region image.

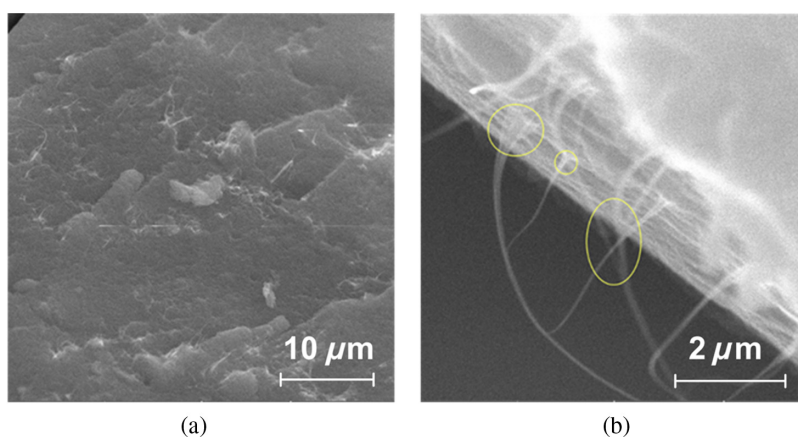


Fig. 8 SEM image of (a) the composite surface and (b) its lateral surface of the composite fraction after grinding.

Next, the powder fractions were glued to an electrically conductive carbon tape and purged with nitrogen. Figure 7 shows the images of stretched elements of the sample in the area of its fracture. The SWCNTs are clearly distinguishable in this image. The yellow ellipses also indicate the SWCNTs binding regions in the volume of the nanocomposite obtained by laser irradiation. It can be seen on SEM images that the effect of SWCNTs binding to the framework structure prevents the destruction of the composite.

The surface of the composite before grinding is shown in Fig. 8(a). The lateral surface of a single composite fraction is shown in Fig. 8(b). The image shows interconnected carbon nanotubes. A greater number of uniformly distributed SWCNTs were observed inside the composite than on its surface.

Hardness and elastic modulus measurements were carried out using a NanoScan-4D Compact nanohardness tester. For the studies, an indenter of the Berkovich type was used. It was a trihedral pyramid with an angle between the axis of the pyramid and a side plane of 65.3 deg (equivalent to a cone angle of 70.32 deg). The radius of curvature of the indenter tip was <math><100\text{ nm}</math>. Indentation was performed at 10 different points with a distance between them of 100 μm . The indentation load was 60 mN. The average values of hardness and elastic modulus were 0.26 ± 0.02 and 5.90 ± 0.035 GPa, respectively. In comparison, human bone has a hardness of ~ 0.48 GPa.

4 Discussion

Under the action of radiation in continuous mode, the sample is heated and, when a temperature of about 45°C is reached, the curing process begins. Under the influence of pulsed radiation with high intensity, but at a low pulse repetition rate, a different picture is observed. This interaction is initially nonlinear at the selected power while nonlinear processes only increase with increasing temperature.³³ Also, as in the case of CW laser, absorption is mainly caused by the presence of nanotubes, while they are capable of intense heat dissipation.³⁴ Therefore, SWCNTs, placed in a liquid medium, can quickly exchange heat with the environment, which leads to their rapid cooling. Composite formation was previously found to be possible using intense femtosecond laser radiation with a wavelength of 810 nm and pulse repetition rate of 80 MHz.²⁶ During such irradiation, a framework of SWCNTs forms, despite the fact that the temperature of the sample does not reach the boiling point of the water, the nanotubes can heat up at high temperatures and reach ~ 1200 K.²⁶

The stickiness of nanotubes was studied without a liquid component in the form of an array.³⁵ This process of laser welding of nanotubes depends on the parameters of the radiation; it was established that at the same power, but at a different wavelength of the laser radiation, the morphology changes in different ways.³⁶ However, an increase in the stickiness quality occurs with an increase in the duration of irradiation at wavelength of 1064 nm. This process is accompanied by

an increase in their graphitization.³⁷ Such process is sensitive to the type of substrate,³⁸ in addition, the nanotubes provide a reliable connection with other materials that can be used in the composite under the action of laser radiation.^{39,40} It can be considered that, mainly, thermal melting occurs, but these experimental data confirm the effect of other processes, namely, chemical and ionic effects, which promote the adhesion of polymer chains.⁴¹

The laser welding process, which can be identified in the case of arrays, is much more difficult to detect in the case of a gelled medium since, in this case, the formation of SWCNT framework occurs in 3-D material. Under the constant action of laser radiation or pulses with a high repetition rate, the composite grows with increasing volume due to the attachment of other nanotubes forming a framework, and the surface of the nanotubes is modified as a result of interaction with albumin⁴² by analogy with a linear polymer.⁴³ However, albumin belongs to the class of globular proteins; therefore, its interaction with a nanotube is more complicated.⁴⁴ It is known that this process is accompanied by conformational changes in albumin during their interaction with SWCNTs.⁴⁵ In accordance with the obtained experimental data, such changes occur upon irradiation with continuous laser radiation at a temperature of $\sim 45^{\circ}\text{C}$ (Fig. 3). Moreover, the process of SWCNTs sticking occurs only after a certain exposure time from the beginning of conformational changes in albumin and is accompanied by an increase in temperature from 45°C to 50°C . In this work, it is shown that the sample can be formed not only with a horizontal arrangement but also on the inner surface of the cuvette due to microroughness. This observation confirms the presence of SWCNT framework and indicates that although water evaporation occurs, but it does not play a major role in this process. The mechanisms of heat transfer in this dispersed medium can be different,⁴⁶ the dominant contribution is the formation of new clusters of nanoparticles. The influence of pulsed radiation with a frequency of 10 Hz at high intensity leads to the manifestation of nonlinear interaction; however, its action can be reduced to the sticking of nanotubes, which are at a fairly close distance from each other at the moment of pulse passage or do not have time to lose heat until the moment of collision between nanotubes during Brownian movement. Since the pulse repetition rate is small, such small adhesions only lead to an increase in particle size and, consequently, to their precipitation. Herewith, the darkening of the lower region in Fig. 5(b) in comparison with the color of the initial sample in Fig. 5(a) may be associated with an increase in the concentration of SWCNTs in this area.⁴⁷ This also indicates the formation of agglomerates of nanotubes, which begin to accumulate in the lower layers. Thus, it can be considered that not only the energy parameters of radiation are important but also the frequency of energy portions exposure.

5 Conclusion

Tissue-engineered structure was fabricated by CW laser radiation. The curing of an aqueous dispersed medium with albumin 20% (w/w) and carbon nanotubes 0.01% (w/w) [Fig. 6(a)] occurred in 660 s at power of ~ 500 mW and wavelength of 532 nm [Fig. 6(c)]. Under the influence of pulsed laser radiation of the same power and duration of 16 ns, a different effect was observed. The composite did not form, and the pulse intensity reached 138.89 MW/cm², which exceeds the threshold value of 0.487 MW/cm² and is characterized by a nonlinear interaction with the substance. In accordance with the results shown in Fig. 6(b), we can conclude that upon irradiation in pulsed mode, the nanotubes stuck and formed the agglomerates (clusters) that have time to precipitate in the interval between pulses. Figure 6(b) shows clearly visible enlightenment above the site of irradiation, and the temperature did not rise above $\sim 40^{\circ}\text{C}$, which also indicates the leaving of the heated particles from irradiation zone. In accordance with the time dependence of normalized transmission (Fig. 5), when compared with the time dependence of temperature (Fig. 4), curing occurred at a temperature of $\sim 45^{\circ}\text{C}$. In previous work, it was shown that composites can be obtained at higher heating of material using pulsed laser radiation at a wavelength of 810 nm and pulse repetition rate of 80 MHz.²⁶ The main influence on the curing process is exerted precisely by the conditions that are necessary for the formation of SWCNT framework, and evaporation does not play the main role. The advantage of using laser radiation of the visible or infrared range is due to the minimal absorption of such radiation by albumin, as a result of which there is minimal impact on its structure.

Acknowledgments

This study was supported by the Russian Science Foundation, Project No. 20-49-04404. The studies were performed using MIET Core facilities center MEMS and electronic components and Sechenov University Grant. There are no relevant financial interests in the manuscript and no other potential conflicts of interest to disclose.

References

1. H. Fan et al., "Fabrication, mechanical properties, and biocompatibility of graphene-reinforced chitosan composites," *Biomacromolecules* **11**(9), 2345–2351 (2010).
2. J. Wang and W. J. Blau, "Nonlinear optical and optical limiting properties of individual single-walled carbon nanotubes," *Appl. Phys. B* **91**(3–4), 521–524 (2008).
3. J. E. Valentin et al., "Functional skeletal muscle formation with a biologic scaffold," *Biomaterials* **31**(29), 7475–7484 (2010).
4. B. M. Sicari et al., "A murine model of volumetric muscle loss and a regenerative medicine approach for tissue replacement," *Tissue Eng. Part A* **18**(19–20), 1941–1948 (2012).
5. K. Dave and V. G. Gomes, "Interactions at scaffold interfaces: effect of surface chemistry, structural attributes and bioaffinity," *Mater. Sci. Eng. C* **105**, 110078 (2019).
6. P. Asuri et al., "The protein–nanomaterial interface," *Curr. Opin. Biotechnol.* **17**(6), 562–568 (2006).
7. P.-S. Li et al., "A novel albumin-based tissue scaffold for autogenic tissue engineering applications," *Sci. Rep.* **4**(1), 5600 (2015).
8. A. Y. Gerasimenko et al., "A study of preparation techniques and properties of bulk nanocomposites based on aqueous albumin dispersion," *Opt. Spectrosc.* **115**(2), 283–289 (2013).
9. B. I. Yakobson and P. Avouris, "Mechanical properties of carbon nanotubes," in *Carbon Nanotubes*, M. S. Dresselhaus, G. Dresselhaus, and P. Avouris, Eds., pp. 287–327, Springer, Berlin, Heidelberg (2001).
10. F. Alvarez-Primo et al., "Fabrication of surfactant-dispersed HiPco single-walled carbon nanotube-based alginate hydrogel composites as cellular products," *Int. J. Mol. Sci.* **20**(19), 4802 (2019).
11. R. Eivazzadeh-Keihan et al., "Carbon based nanomaterials for tissue engineering of bone: building new bone on small black scaffolds: a review," *J. Adv. Res.* **18**, 185–201 (2019).
12. M. Chen, X. Qin, and G. Zeng, "Biodegradation of carbon nanotubes, graphene, and their derivatives," *Trends Biotechnol.* **35**(9), 836–846 (2017).
13. K. K. Bokara et al., "Biocompatibility of carbon nanotubes with stem cells to treat CNS injuries," *Anat. Cell Biol.* **46**(2), 85–92 (2013).
14. A. Huczko and H. Lange, "Carbon nanotubes: experimental evidence for a null risk of skin irritation and allergy," *Fullerene Sci. Technol.* **9**(2), 247–250 (2001).
15. S. K. Smart et al., "The biocompatibility of carbon nanotubes," *Carbon* **44**(6), 1034–1047 (2006).
16. N. Saito et al., "Carbon nanotubes: biomaterial applications," *Chem. Soc. Rev.* **38**(7), 1897–1903 (2009).
17. L. P. Krul et al., "Nanocomposites based on poly-D, L-lactide and multiwall carbon nanotubes," *Biomol. Eng.* **24**(1), 93–95 (2007).
18. B. S. Harrison and A. Atala, "Carbon nanotube applications for tissue engineering," *Biomaterials* **28**(2), 344–353 (2007).
19. Y. Zhao et al., "Hemocompatibility of electrospun halloysite nanotube- and carbon nanotube-doped composite poly(lactic-co-glycolic acid) nanofibers," *J. Appl. Polym. Sci.* **127**(6), 4825–4832 (2013).
20. T. V. Vakhrusheva et al., "Albumin reduces thrombogenic potential of single-walled carbon nanotubes," *Toxicol. Lett.* **221**(2), 137–145 (2013).
21. J. Meng et al., "Effects of single-walled carbon nanotubes on the functions of plasma proteins and potentials in vascular prostheses," *Nanomed. Nanotechnol. Biol. Med.* **1**(2), 136–142 (2005).

22. U. E. Kurilova et al., "Spectral studies of biodegradation and hemolysis caused by contact of bulk and film nanocomposites with biological fluids," *Biomed. Eng.* **51**(1), 16–19 (2017).
23. H.-Y. Mi et al., "Carbon nanotube (CNT) and nanofibrillated cellulose (NFC) reinforcement effect on thermoplastic polyurethane (TPU) scaffolds fabricated via phase separation using dimethyl sulfoxide (DMSO) as solvent," *J. Mech. Behav. Biomed. Mater.* **62**, 417–427 (2016).
24. S. Derakhshanfar et al., "3D bioprinting for biomedical devices and tissue engineering: a review of recent trends and advances," *Bioact. Mater.* **3**(2), 144–156 (2018).
25. L. Elomaa et al., "Three-dimensional fabrication of cell-laden biodegradable poly(ethylene glycol-co-depsipeptide) hydrogels by visible light stereolithography," *J. Mater. Chem. B* **3**(42), 8348–8358 (2015).
26. A. Y. Gerasimenko et al., "Laser structuring of carbon nanotubes in the albumin matrix for the creation of composite biostructures," *J. Biomed. Opt.* **22**(6), 065003 (2017).
27. M. S. Savelyev et al., "Investigation of albumin denaturation when exposed to a nanosecond laser source," *AIP Conf. Proc.* **2140**, 020063 (2019).
28. Z. Wang et al., "A simple and high-resolution stereolithography-based 3D bioprinting system using visible light crosslinkable bioinks," *Biofabrication* **7**(4), 045009 (2015).
29. D. Li et al., "An automated 3D visible light stereolithography platform for hydrogel-based micron-sized structures," *AIP Adv.* **9**(6), 065204 (2019).
30. A. Y. Gerasimenko et al., "Investigation of the nonlinear properties of carbon nanomaterials for thresholding of powerful laser radiation," *Biomed. Eng.* **48**(6), 324–327 (2015).
31. M. S. Savelyev et al., "Conjugates of thermally stable phthalocyanine J-type dimers with single-walled carbon nanotubes for enhanced optical limiting applications," *Opt. Laser Technol.* **117**, 272–279 (2019).
32. M. S. Savelyev et al., "Nonlinear optical characteristics of albumin and collagen dispersions with single-walled carbon nanotubes," *Mater. Phys. Mech.* **37**(2), 133–139 (2018).
33. R. Y. Krivenkov et al., "Heat-induced dip of optical limiting threshold in carbon nanotube aqueous suspension," *J. Phys. Chem. C* **122**(28), 16339–16345 (2018).
34. A. Tan et al., "Synergistic photothermal ablative effects of functionalizing carbon nanotubes with a POSS-PCU nanocomposite polymer," *J. Nanobiotechnol.* **10**(1), 34 (2012).
35. A. Y. Gerasimenko et al., "Influence of laser structuring and barium nitrate treatment on morphology and electrophysical characteristics of vertically aligned carbon nanotube arrays," *Diamond Relat. Mater.* **96**, 104–111 (2019).
36. Y. Yuan and J. Chen, "Morphology adjustments of multi-walled carbon nanotubes by laser irradiation," *Laser Phys. Lett.* **13**(6), 066001 (2016).
37. Y. Yuan et al., "Nanoscale welding of multi-walled carbon nanotubes by 1064 nm fiber laser," *Opt. Laser Technol.* **103**, 327–329 (2018).
38. Y. Yuan and J. Chen, "Nano-welding of multi-walled carbon nanotubes on silicon and silica surface by laser irradiation," *Nanomaterials* **6**(3), 36 (2016).
39. Y.-T. Liu et al., "Laser welding of carbon nanotube networks on carbon fibers from ultrasonic-directed assembly," *Mater. Lett.* **236**, 244–247 (2019).
40. J. B. In et al., "Laser welding of vertically aligned carbon nanotube arrays on polymer workpieces," *Carbon* **115**, 688–693 (2017).
41. A. M. Visco et al., "Effect of carbon nanotube amount on polyethylene welding process induced by laser source," *Appl. Phys. A* **103**(2), 439–445 (2011).
42. K. Lou et al., "Comprehensive studies on the nature of interaction between carboxylated multi-walled carbon nanotubes and bovine serum albumin," *Chem. Biol. Interact.* **243**, 54–61 (2016).
43. M. J. O'Connell et al., "Reversible water-solubilization of single-walled carbon nanotubes by polymer wrapping," *Chem. Phys. Lett.* **342**(3–4), 265–271 (2001).
44. K. Nagaraju, R. Reddy, and N. Reddy, "A review on protein functionalized carbon nanotubes," *J. Appl. Biomater. Funct. Mater.* **13**(4), e301–e312 (2015).
45. G. N. Ten et al., "Interpretation of IR and Raman Spectra of Albumin," *Izv. Saratov Univ. New Ser. Ser. Phys.* **19**(1), 43–57 (2019).

46. V. I. Terekhov, S. V. Kalinina, and V. V. Lemanov, "The mechanism of heat transfer in nanofluids: state of the art (review). Part 1. Synthesis and properties of nanofluids," *Thermophys. Aeromechanics* **17**(1), 1–14 (2010).
47. T. Hasan et al., "Stabilization and 'Debundling' of single-wall carbon nanotube dispersions in N-methyl-2-pyrrolidone (NMP) by polyvinylpyrrolidone (PVP)," *J. Phys. Chem. C* **111**(34), 12594–12602 (2007).

Mikhail S. Savelyev is an associate professor at the National Research University of Electronic Technology, MIET. He received his PhD in condensed-matter physics from the MIET in 2016. Since 2018, he has been working as a senior researcher at Sechenov University. He is the author of more than 40 journal papers and has written one book chapter. His current research interests include investigating the fundamental mechanisms and applications of nonlinear optical processes. He is a member of SPIE.

Natalia O. Agafonova is a master's student at the National Research University of Electronic Technology, MIET. She received her bachelor's degree in biotechnological systems and technologies from MIET in 2018. She is the coauthor of six publications. Her main research focus is protein denaturation processes when exposed to a laser pulse.

Pavel N. Vasilevsky is a postgraduate student at the National Research University of Electronic Technology. He received his BS and MS degrees from the MIET in 2017 and 2019, respectively. He is the author of more than 10 journal papers. His current research interests include investigating the interaction of laser radiation with dispersed media, including biocompatible media, as well as nonlinear optical effects. He is a member of SPIE.

Dmitry I. Ryabkin is an engineer at the National Research University of Electronic Technology, MIET. He received his master's degree in electronics and nanoelectronics from the MIET in 2015. He is the author of more than five journal papers. His current research interests include the modeling and applications of laser welding of biological tissues. He is a member of SPIE.

Dmitry V. Telyshev received his BS, MS, and PhD degrees from the National Research University of Electronic Technology, Moscow, Russia, in 2006, 2008, and 2011, respectively, all in electronic engineering. He is currently the director of the Institute for Bionic Technologies and Engineering, Sechenov First Moscow State Medical University, Moscow, Russia, and an associate professor with the Institute of Biomedical Systems, National Research University of Electronic Technology. He has authored and coauthored about 70 technical papers. His research interests include the design of mechanical circulatory support systems and general problems of design of implantable medical devices.

Peter S. Timashev graduated from the Lomonosov Moscow State University of Fine Chemical Technologies. In 2004, he received his PhD in solid-state chemistry from Karpov Institute of Physical Chemistry and became a DSc in 2016. He is the director of the Institute for Regenerative Medicine and the head of the Department for Advanced Biomaterials, Sechenov University, Moscow, Russia. He is the author of more than 160 publications and eight patents (RU) and a laureate of the Moscow Government Prize in 2017.

Alexander Yu. Gerasimenko is an associate professor at the National Research University of Electronic Technology MIET and head of the Biomedical Nanotechnology Laboratory I.M. Sechenov First Moscow State Medical University. He received his PhD in condensed-matter physics in 2010. He is the author of more than 70 journal papers and has written 5 book chapters and 3 study guides. His current research interests include optoelectronic biomedical systems as well as interaction of radiation with nanomaterials and biopolymers. He is a member of SPIE and advisor of the SPIE student chapter.